

Published in final edited form as:

*Cell*. 2011 April 15; 145(2): 183–197. doi:10.1016/j.cell.2011.03.003.

## Wdr5 mediates self-renewal and reprogramming via the embryonic stem cell core transcriptional network

Yen-Sin Ang<sup>1,2,3,#</sup>, Su-Yi Tsai<sup>1,3,5</sup>, Dung-Fang Lee<sup>1,2,3,\*</sup>, Jonathan Monk<sup>1,2,\*</sup>, Jie Su<sup>1,2,3,\*</sup>, Kajan Ratnakumar<sup>1,4,5</sup>, Junjun Ding<sup>1,3</sup>, Yongchao Ge<sup>6</sup>, Henia Darr<sup>1,2,3</sup>, Betty Chang<sup>1,2,3</sup>, Jianlong Wang<sup>1,3</sup>, Michael Rendl<sup>1,3,5</sup>, Emily Bernstein<sup>1,4,5,\*</sup>, Christoph Schaniel<sup>1,2,\*</sup>, and Ihor R. Lemischka<sup>1,2,3,#</sup>

<sup>1</sup>Black Family Stem Cell Institute, Mount Sinai School of Medicine, New York, New York, USA

<sup>2</sup>Department of Gene and Cell Medicine, Mount Sinai School of Medicine, New York, New York, USA

<sup>3</sup>Department of Developmental and Regenerative Biology, Mount Sinai School of Medicine, New York, New York, USA

<sup>4</sup>Department of Oncological Sciences, Mount Sinai School of Medicine, New York, New York, USA

<sup>5</sup>Department of Dermatology Mount Sinai School of Medicine, New York, New York, USA

<sup>6</sup>Department of Neurology, Mount Sinai School of Medicine, New York, New York, USA

### SUMMARY

The embryonic stem (ES) cell transcriptional and epigenetic networks are critical for the maintenance of ES cell self-renewal. However, it remains unclear whether components of these networks functionally interact and if so, what factors mediate such interactions. Here we show that WD-repeat protein-5 (Wdr5), a core member of the mammalian Trithorax (*trxG*) complex, positively correlates with the undifferentiated state and is a novel regulator of ES cell self-renewal. We demonstrate that Wdr5, an ‘effector’ of H3K4 methylation, interacts with the pluripotency transcription factor Oct4. Genome-wide protein localization and transcriptome analyses demonstrate overlapping gene regulatory functions between Oct4 and Wdr5. We show that the Oct4-Sox2-Nanog circuitry and *trxG* cooperate in activating transcription of key self-renewal regulators. Furthermore, Wdr5 expression is required for the efficient formation of induced

© 2011 Elsevier Inc. All rights reserved.

#Correspondence should be addressed to: Ihor R. Lemischka, Ph.D., Mount Sinai School of Medicine, Department of Gene & Cell Medicine, 1425 Madison Ave, Icahn 13-20F, New York, NY-10029, USA, Phone: 1-212-659-8228, [ihor.lemischka@mssm.edu](mailto:ihor.lemischka@mssm.edu), or Yen-Sin Ang, Mount Sinai School of Medicine, Department of Gene & Cell Medicine, 1425 Madison Ave, Icahn 13-26C, New York, NY-10029, USA, Phone: 1-212-659-8251, [yen-sin.ang@mssm.edu](mailto:yen-sin.ang@mssm.edu).

\*These authors contributed equally and were placed by last names

**Publisher's Disclaimer:** This is a PDF file of an unedited manuscript that has been accepted for publication. As a service to our customers we are providing this early version of the manuscript. The manuscript will undergo copyediting, typesetting, and review of the resulting proof before it is published in its final citable form. Please note that during the production process errors may be discovered which could affect the content, and all legal disclaimers that apply to the journal pertain.

### SUPPLEMENTARY INFORMATION

Supplemental Information includes Extended Experimental Procedures, seven supplemental figures, and six tables available with the online version.

Author Contributions: YS-Ang: conception and design, collection and analysis of data, manuscript writing, final approval of manuscript; SY-Tsai, DF-Lee, J-Monk, J-Su, K-Ratnakumar, J-Ding, YC-Ge, H-Darr: collection and analysis of data; J-Wang, B-Chang, M-Rendl: manuscript writing; E-Bernstein: conception and design, manuscript writing; C-Schaniel: conception and design, data collection and manuscript writing; I-Lemischka: conception and design, financial support, manuscript writing, final approval of manuscript.

pluripotent stem (iPS) cells. We propose an integrated model of transcriptional and epigenetic control, mediated by select *trxG* members, for maintenance of ES cell self-renewal and somatic cell reprogramming.

### Keywords

embryonic stem; histone methylation; trithorax; induced pluripotent stem; reprogramming; wdr5; chromatin; transcriptional network; Oct4

## INTRODUCTION

The maintenance of ES cell self-renewal requires a network of transcription factors including Oct4, Sox2, Nanog, Esrrb, Tbx3 and Tcf3 (Chen et al., 2008; Ivanova et al., 2006; Kim et al., 2008; Tam et al., 2008). These factors participate in auto- and cross-regulatory interactions to increase their own expression and that of other self-renewal associated genes, while repressing genes that promote differentiation. Perturbation of these factors collapses the self-renewal circuitry and triggers specific or mixed lineage differentiation (Ivanova et al., 2006). In contrast to the numerous transcription factors, only a handful of chromatin regulators important for self-renewal have been characterized (Loh et al., 2007; Pasini et al., 2007; Schaniel et al., 2009).

ES cells harbor an open, transcriptionally permissive chromatin that allows for efficient epigenomic remodeling during lineage commitment (Efroni et al., 2008). However, factors regulating this ‘hyperdynamic’ epigenetic configuration remain poorly understood. ES cells also contain “bivalent domains” where nucleosomes are marked by tri-methylation at histone3-lysine27 (H3K27me3) and histone3-lysine4 (H3K4me3) (Bernstein et al., 2006). The Polycomb Group (*PcG*) complex mediate H3K27me3, correlated with gene repression (Boyer et al., 2006). In contrast, the Trithorax Group (*trxG*) complex mediate H3K4me3, generally correlated with gene activation (Ringrose and Paro, 2004). While *PcG* have been extensively investigated in the maintenance of ES cell self-renewal, pluripotency and somatic cell reprogramming, there exists little complementary information for *trxG*-associated members. This imbalance of knowledge represents a significant shortcoming in the understanding of the roles played by tri-methylated H3K4 and H3K27 in regulating the ES cell identity. Moreover, it remains to be shown whether the well-established transcriptional network can functionally interact with epigenetic regulators to maintain pluripotency and more importantly which factors mediate such interactions.

An unresolved question in chromatin biology is the manner by which generic histone modification complexes, like *PcG* and *trxG*, become targeted to specific genomic loci to direct specific gene regulatory functions (Schuettengruber et al., 2007). This is especially intriguing in the context of ES cells. For example Chd1, a Chromodomain-helicase-DNA-binding protein that is not specific to ES cells, was recently described to be essential for pluripotency and reprogramming (Gaspar-Maia et al., 2009). The factor(s) or mechanism(s) conferring such functional specificity to epigenetic regulators remains unknown. Moreover, it is unclear how ectopic expression of four transcription factors - Oct4, Sox2, Klf4 and c-Myc (OSKM) can reprogram somatic cells to iPS cells with epigenomes largely indistinguishable from ES cells (Carvajal-Vergara et al., 2010; Tsai et al., 2010). This is especially pertinent to the re-establishment of the bivalent signature. Interestingly, although the OSKM-iPS methodology has been replaced by various combinations of factors or small molecules, Oct4 remains the sole factor that until recently, could not be substituted/omitted (Heng et al., 2010). Accordingly, we reasoned that the resetting of the somatic epigenome must be achieved through the activity of Oct4 interacting proteins and/or Oct4 target genes.

Protein complexes of the Set/MLL histone methyltransferase (HMT) family are mammalian homologues of *trxG* that function as conserved, multi-subunit ensembles to catalyse the methylation of H3K4. The human *MLL* gene, which contains a SET domain, was first identified based on translocations commonly associated with the pathogenesis of multiple forms of hematological malignancies (Shilatifard, 2006). Notably, Set/MLL proteins alone are catalytically inactive, but require core subunits- Wdr5, Ash21 and Rbbp5, that are related to components of the yeast Set1 complex (Dou et al., 2006). The Rbbp5 and Ash21 heterodimer directly participates in HMT activity of the MLL1 complex (Cao et al., 2010). Ash21 is required for mouse embryogenesis (Taylor et al., 2010) and proper X-inactivation (Pullirsch et al., 2010), while diminished recruitment of Rbbp5 is found in patients with Wiskott-Aldrich syndrome (Stoller et al., 2010). Other *trxG*-associated co-factors such as Menin, Hcf1 and Cxxc1, have been implicated in processes like pancreatic  $\beta$ -cell growth (Karnik et al., 2007), tumorigenesis (Lairmore and Chen, 2009), apoptosis (Tyagi and Herr, 2009) and euchromatin formation (Thomson et al., 2010). In particular, Wdr5 is a key component of *trxG* acting as a “presenter” of the H3K4 residue and is indispensable for Set/MLL complex assembly and effective HMT activity (Dou et al., 2006). It was shown that Wdr5 interacts with H3K4me2 and mediates transition to the tri-methylated state (Wysocka et al., 2005). However, it was also shown that Wdr5 is unable to distinguish between different H3K4-methylation states (Couture et al., 2006). While Wdr5 function is required for vertebrate development (Wysocka et al., 2005) and osteoblast differentiation (Zhu et al., 2008), its role in ES or iPS cells remains to be determined.

## RESULTS

### Wdr5 expression positively correlates with the undifferentiated ES cell state

We sought to functionally characterize specific chromatin-regulators in the maintenance of ES cell self-renewal with a particular focus on *trxG*-associated members. For this, we mined our previous microarray data (Ivanova et al., 2006) and published iPS cell datasets for expressions of *trxG* complex members. Wdr5 emerged as an obvious candidate as its expression was down-regulated upon differentiation (Figure 1A) and up-regulated during iPS cell formation (Figure S1A); unlike other members whose expression levels were incoherent among the datasets. Interestingly, the up-regulation of Wdr5 in iPS cells was independent of the somatic cell types chosen for reprogramming. We also observed higher Wdr5 and H3K4me3 levels in ES cells than in somatic cells and tissues (Figure S1B, C), suggesting specific Wdr5 functions in ES and iPS cell maintenance.

We next validated our microarray data and observed marked a Wdr5 reduction, similar to Oct4 and Nanog, with concomitant decreases in global H3K4me3 (Figure 1B). Wdr5 diminution in embryoid body (EB) assays indicated that this was not specific to retinoid acid (RA)-induction but generally representative of differentiation (Figure 1C). Additionally, when we depleted Oct4 or Nanog using short hairpin-RNA (shRNA), we also observed a reduction in Wdr5 (Figure 1D). This effect was not unique to the shRNAs as Wdr5 decreases were also observed using the Nanog-inducible and Oct4-repressible ES cell lines (Figure 1E). Furthermore, chromatin immunoprecipitation (ChIP) confirmed Oct4 and Nanog occupancy in intron 1 of *Wdr5* (Figure 1F). These data indicate that Wdr5 expression correlates positively with the undifferentiated state and that the *Wdr5* gene is a downstream target of Oct4 and Nanog.

### Wdr5 is a novel regulator of ES cell self-renewal

We next designed shRNAs targeting Wdr5 to determine if it is required for self-renewal. Wdr5 shRNA-2 and -4 effectively depleted Wdr5 mRNA and protein levels but not those encoding other WD-repeat proteins (Figure 2A, Figure S1D). Wdr5-knockdown induced

changes in cell morphology and decreased alkaline phosphatase (AP) activity, indicative of differentiation (Figure 2B). In ES cell competition assays, Wdr5 depletion resulted in loss of self-renewal similar to depletion of LIF receptor (LIFR) or Nanog (Figure 2C). Furthermore, depletion of Wdr5 diminished secondary ES colony formation (Figure 2D) and reduced self-renewal gene expression while increasing ectodermal and trophectodermal gene expressions (Figure S1E). Importantly, Wdr5 depletion induced the collapse of the extended ES cell transcriptional network (Figure 2E).

To rule out shRNA off-target effects, we built complementation 'rescue' ES cell lines (Wdr5R) where endogenous Wdr5 was constitutively repressed by Wdr5-shRNA and rescued by a Doxycycline-inducible (Dox) shRNA-immune Wdr5 (Figure 2F). Removal of Dox resulted in loss of self-renewal gene expression in two independent clones; whereas, in the presence of Dox, expression remained at normal levels. This was also evident from AP staining (Figure S2A). Global gene expression profiling and Gene Set Enrichment Analyses (GSEA) demonstrated that Wdr5 depletion repressed self-renewal and enhanced primarily ectoderm differentiation (Figure 2G, Figure S2B). Gene Ontology (GO) analysis of the differentially expressed genes revealed enrichment in categories like developmental processes, mesoderm and skeletal development, and others (Figure S2C). Arguing against induced apoptosis or a general loss of proliferative potential, Wdr5-depletion in ES cells resulted in no change in apoptotic gene expressions while cell cycle analysis showed only a marginal impediment (Figure S2D, E). Indeed, sporadic clusters of viable cells expressing lineage-specific markers, nestin and smooth muscle actin, were detectable after extended periods of Wdr5-knockdown (Figure S2F). Additionally, Wdr5-depletion in fibroblasts and myoblasts, induced no significant changes in cell cycle suggesting that Wdr5 has specific roles in maintenance of ES cell self-renewal (Figure S2G–I).

We next asked if Wdr5 over-expression was sufficient to block differentiation in EB-assays using the Wdr5R (Figure S2J). Wdr5 over-expression (+Dox) delayed trophectoderm and mesoderm differentiation (Figure S2K, L); enhanced endoderm differentiation (Figure S2N), but failed to prevent loss of self-renewal genes (Figure S2O). Conversely, Wdr5 repression enhanced commitment to trophectoderm and endoderm yet accelerated the loss of self-renewal markers (Figure S2K, N, O). The enhanced differentiation following knockdown of Wdr5 also argues against a general loss of cell viability. Finally, transient over-expression of Wdr5 under self-renewing conditions resulted in no change in ES cell identity (data not shown). Collectively, these results show that Wdr5 plays specific roles in maintaining an intact ES cell transcriptional network and consequently, a self-renewal phenotype but is insufficient to block differentiation.

### **Wdr5 maintains global and localized H3K4 tri-methylation**

We further pursued the mechanism by which Wdr5 regulates self-renewal. Wdr5 is known to be required for H3K4me3 modification and HOX gene activation (Wysocka et al., 2005). As expected, Wdr5 knockdown reduced the amount of Wdr5 in chromatin and global H3K4me3 levels (Figure 3A). Moreover, we observed that the reduction in H3K4me3 precedes down-regulation of Oct4, Nanog or SSEA1 markers (Figure 2F, left). At 2 days after Wdr5-depletion, while no change in Oct4 or Nanog levels was detectable, H3K4me3 levels was evidently reduced by more than 50%. This diminution continued where it became more marked at day 4. We reason that H3K4me3-reduction is even more significant at day 4, after the initiation of Oct4 down-regulation, because *Wdr5* is a downstream target gene of Oct4. Thus, depletion of Oct4 could further attenuate the transcription of Wdr5, and consequently expression levels of global H3K4me3. Additionally, a significant SSEA1 decrease was only detected after day 3 (Figure S3A). These data indicate that loss of H3K4me3 is a direct result of Wdr5-depletion and not an indirect result of the loss of pluripotency factors such as, Oct4 or Nanog.

We further detected decreases in H3K4me3 at the *Pou5f1* and *Nanog* loci upon Wdr5-depletion (Figure 3B). H3K4me3 reduction also occurred at pluripotency-associated gene promoters where we had shown decreased expression levels (Figure 3C), as well as at ‘bivalent’ promoters, and at other promoters (Figure S3B). In line with the role of H3K4me3 in RNA polymerase II (RNAP-II) recruitment (Wang et al., 2009), Wdr5 loss reduced RNAP-II occupancy at *Nanog*, *Sox2*, *Fbx15* and *Myc* genes (Figure 3D). Moreover, using a Nanog-reporter line (Schaniel et al., 2009), Wdr5 depletion reduced Nanog promoter activity (Figure S3C). Knockdowns of two other *trxG*-associated members Ash2l and Menin (Shilatifard, 2006) also induced ES cell differentiation (Figure S3D). This strongly suggested that the maintenance of self-renewal requires elevated H3K4me3 expression. Collectively, these data indicate that Wdr5 is critical for the maintenance of global and localized H3K4me3 and for transcriptional activation in ES cells.

### Wdr5 interacts with Oct4 in ES cells

The indispensable role of Wdr5 in self-renewal suggested probable physical interactions with components of the core transcriptional network. Co-immunoprecipitation (co-IP) using an Oct4 antibody demonstrated an interaction with Wdr5 (Figure 4A). To confirm the Wdr5-Oct4 interaction, we derived ES cell lines where Wdr5 was tagged with Flag or Myc epitopes and selected for clones that had minimum Wdr5 over-expression (Figure S4A). Additionally, we measured self-renewal and differentiation markers to pick clones that were statistically indistinguishable from the control line (Figure S4B). A resultant Wdr5\_FL2 line had typical growth rates and morphology and was capable of *in vitro* and *in vivo* differentiation (Figure S4D–F); demonstrating *bona fide* pluripotency. Using this line, we successfully co-IP’ed Wdr5 with Oct4 (Figure 4A); as well as Nanog and Sox2 (data not shown). Co-IP of other *trxG*-associated members, Rbbp5 and Menin, suggested that these factors exist in functionally-active protein complexes. We next performed a gel filtration experiment to ask if Oct4 is part of the larger *trxG*-complex (Figure 4B). We observed that while Oct4 is enriched primarily at molecular weight (MW) fractions between 150-50kDa and Wdr5, Ash2l, Rbbp5 are enriched primarily at >600kDa MW fractions, there were several fractions where substantial amounts of Oct4 co-eluted with the core *trxG*-associated proteins (Figure 4B, orange box). Interestingly, we also observed Wdr5 to be the major protein co-eluting at peak Oct4 fractions, in the absence of Ash2l or Rbbp5 (Figure 4B, blue). This suggests that the Wdr5-Oct4 partnership might extend beyond HMT activity alone.

We continued to validate the Wdr5-Oct4 interaction using epitope-tagged proteins expressed in 293T cells (Figure 4C). Oct4-IP successfully pulled-down Wdr5 while the reciprocal IP was less efficient; presumably because Wdr5 gets competed away by endogenous interacting partners. We also performed an *in vitro* binding assay using recombinant Wdr5 and Oct4 (Figure 4D). Encouragingly, we observed co-IP of recombinant-Wdr5 using an antibody specific for Oct4. However, this pull-down was significantly weaker than in co-IPs in ES or 293T cells; suggesting that while Wdr5 and Oct4 are direct interaction partners, the interaction might be further stabilized in a multimeric complex.

It was shown previously that strong Myc-DNA binding is positively correlated with ‘euchromatic clusters’ that bear high H3K4me3 levels (Guccione et al., 2006). Therefore, we hypothesized that Oct4 binding to DNA may also be dependent on certain epigenetic features and be mediated through Wdr5. To investigate this, we performed a sequential peptide-IP experiment (Figure 4E–box). As expected, biotinylated-peptide pulldown assays demonstrated strong Wdr5 specificity toward the H3K4me3 peptide in stringent salt conditions (Figure S4G). Flag-IP of the Wdr5-Oct4 complex (IP1) followed by peptide-IP (IP2) demonstrated specificity of Oct4 for the H3K4me3 peptide. Increased salt concentration retained the specificity of Wdr5 for H3K4me3 but abolished the interaction



with Oct4 (Figure 4E). These data point to indirect interactions of Oct4 with H3K4me3-modified histones, mediated by Wdr5, and suggest that portions of the ES cell genome that are 'visible' to Oct4 could be restricted by higher-order chromatin organization.

### Wdr5 and Oct4 share overlapping gene regulatory functions

What is the functional importance of the Wdr5-Oct4 interaction? We postulated that Oct4 would be required to recruit Wdr5 to self-renewal-associated gene promoters and this in turn, maintains robust H3K4me3. Indeed, Oct4 depletion decreased Wdr5 binding as well as H3K4me3 modification at promoters (*Pou5f1*, *Nanog*, *Sox2*) co-bound by Wdr5 and Oct4 (Figure 4F). In contrast, at genes (*Adfp*, *Gnl3*) bound by Wdr5 but not by Oct4, we detected increased Wdr5 binding and H3K4me3 modification upon Oct4 depletion. This suggests that the Wdr5-Oct4 partnership performs specific roles at promoters of self-renewal genes and Wdr5 also performs discreet transcriptional functions without the participation of Oct4.

To assess the global extent of gene regulation, we compared differentially expressed genes upon depletion of Wdr5 or Oct4 (Table S2). One-thousand five-hundred thirty-two and 646 genes were differentially expressed after Wdr5 or Oct4 knockdown, respectively, with 329 common genes (Figure 4G). Interestingly, GSEA showed high enrichment of Oct4-activated genes in control ES cells that become repressed upon Wdr5 depletion (Figure 4H, Figure S5A). Conversely, Oct4-repressed genes became enriched only upon loss of Wdr5. GSEA comparisons with published ChIP-datasets of bivalent promoters and transcription factor binding targets provided additional evidence that Oct4 and Wdr5 share significant overlapping gene regulatory functions (Figure S5B, C).

### Genome-wide mapping of Wdr5, Rbbp5, H3K4me3, and Oct4 localizations using ChIP-sequencing

To determine the direct transcriptional targets of Oct4 and Wdr5, we mapped the DNA-binding sites for Wdr5 and Oct4, along with Rbbp5 and H3K4me3, by ChIP-sequencing (Figure S6A). Comparison with published H3K4me3- and Oct4-ChIP-seq datasets exhibited strong overlap in target genes and local binding profiles (data not shown), as well as high co-localization frequencies of binding regions (Figure 5D). Importantly, ChIP-qPCR validation revealed a low False Discovery Rate (FDR) for the identified binding regions (Figure S6B).

In support of our earlier observations (Figure 4G, H), the distributions of Oct4 and Wdr5 localization was strikingly similar (Figure 5A, B) where 75% of Oct4 target genes were co-bound by Wdr5 (Figure 5C). In line with a recent report (Kim et al., 2010), clustering of the colocalization frequencies of histone modifications, transcription factors and transcriptional regulatory proteins recapitulated a Polycomb (Figure 5D, blue), ES-Core (red) and Myc modules (green). Evidently, Oct4 and the Core module share no significant overlap with regions of the genome marked by H3K27me3, H3K36me3 or H3K9me3 modifications. As expected, Wdr5 and Oct4 share a strong correlation in their binding regions and serve to bridge the Myc and the Core modules (red-green). Lastly, the top Oct4-bound genes have significantly higher Wdr5 ChIP-seq signals than the bottom Oct4-bound genes (Figure 5E). The converse was also true; providing additional evidence that Oct4 and Wdr5 are partners in transcriptional regulation.

Wdr5, Rbbp5 and H3K4me3 binding regions are largely located within Refseq promoters (Figure 5A), over-represented in gene-rich chromosomal regions (Figure S6C) and share a strong overlap in their binding targets (Figure 6A). We identified 9303 Wdr5, Rbbp5 and H3K4me3 co-associated target genes, termed *trxG* hereafter. In line with the gene-activation role of *trxG* (Ringrose and Paro, 2004), the level of mRNA expression in ES cells was

directly proportional to the intensity of *trxG* ChIP-seq signals (Figure 6B). Lastly, a large proportion of *trxG* target genes contained ‘bivalent’ domains (Table S3, Figure S6D) and GO enrichment in categories like developmental processes, neurogenesis, embryogenesis, mesoderm and ectoderm development (Figure S6E).

### Oct4, Sox2, Nanog and *trxG* cooperate in transcriptional activation

We sought to understand the extent to which the known transcriptional network cooperates with *trxG* in gene regulation, by broadening our analyses to include genes bound by *trxG* as well as Oct4 (this study), Sox2 and Nanog (Marson et al., 2008) (OSN) (Table S1). Oct4, Sox2 and Nanog are known to possess both transcriptional activation and repression functions but the specific mechanisms that distinguish between these two properties remain elusive (Marson et al., 2008). We hypothesized that since *trxG* is required for transcriptional activation (Ringrose and Paro, 2004), it would work with OSN specifically for this function. We identified four markers of active transcription from published reports (Marson et al., 2008; Mikkelsen et al., 2007; Rahl et al., 2010)- H3K79me2, H3K36me3, elongating RNAPII (RNAPII-Ser2P) and Paf1 complex (Ctr9) binding; and a marker of repression-H3K27me3 (Mikkelsen et al., 2007). As described previously (Rahl et al., 2010), cMyc targets are highly positive for all four activation marks, while Suz12 targets are largely H3K27me3 positive (Figure 6C, top). Next, we observed *trxG* and Oct4 targets to be significantly activated above baseline levels. Additionally, target genes with OSN co-occupancy were preferentially more active than targets occupied by Oct4 alone; in line with the hypothesis that these transcription factors act synergistically for gene activation (Kim et al., 2008).

Five sectors, [I]–[V], of genes were identified based on their occupancies by *trxG* and/or OSN (Figure 6D) (Table S3). We then asked what is the percentage of genes in Sectors [I]–[V] containing these marks of activation. Remarkably, the percentage of active genes was highest in sector [I] and was as high as that for cMyc, a strong transcriptional activator (Figure 6C, bottom). In contrast, the percentage of active genes was markedly reduced in the absence of OSN or *trxG* co-occupancies, represented by sectors [II] and [III] respectively. This trend was not observed using the H3K27me3 repressive mark.

What are the properties of the genes in Sector [I], [II], [III] and how do their expressions change upon differentiation? Using GSEA, we observed that: (i) OSN and *trxG* co-bound genes (Sector [I]) represented key self-renewal regulators (eg. *Oct4*, *Nanog*, *Sox2*) that are highly expressed in undifferentiated ES cells as indicated by a highly positive normalized enrichment score (NES) of +1.93 (Figure 6E, Column-1); (ii) OSN without *trxG* co-bound genes (Sector [II]) represented ‘auxiliary’ pluripotency-associated regulators (eg. *Dppa3*, *Fbxo15*, *Gdf3*). This gene-set is not as highly expressed in ES cells as indicated by a lowered NES of +1.59 and might share redundant functions with Sector [I] genes (Figure 6E, Column-2); (iii) *trxG* without OSN co-bound genes (Sector [III]) represented primarily developmental regulators (eg. *Dhx16*, *Hoxa9*, *Tnni1*) that are highly expressed only in differentiated cells as indicated by a highly negative NES of –1.5 (Figure 6E, Column-3). These findings suggest that the OSN transcriptional circuitry and *trxG* are accomplices in transcriptional activation of key self-renewal genes.

### Wdr5 is required for efficient somatic cell reprogramming

It remains unclear how OSKM with no immediate histone modification activities, reconfigure the epigenome during somatic cell reprogramming. Notably, we observed up-regulation of Wdr5 during iPS cell generation (Figure 7A, B) that led us to hypothesize that Oct4 partners with Wdr5 to reset the epigenome during iPS cell formation. Therefore we asked if Wdr5 is indeed required for reprogramming of mouse embryonic fibroblast (MEF)

from Oct4–GFP reporter mice (Figure S7A). Specific down-regulation of Wdr5 in MEFs (Figure S7B) reduced the number of iPS colonies, as scored by colony morphology (Figure S7C), Oct4-GFP expression (Figure 7C) and number of AP positive colonies (Figure 7D). This observation was not due to an adverse effect of Wdr5 depletion on the proliferative capacity of MEFs (Figure 7E, Figure S7D). Our cell cycle analyses in 3T3 fibroblasts further support this observation (Figure 2I). Oct4-GFP positive colonies emerging in the Wdr5 knockdown cultures either had not been infected by the shRNA-lentivirus or had silenced it, as determined by Wdr5 RT-PCR (Figure S7E). We next asked if Wdr5 is required for the early/initiation phase or the later/expansion phase of reprogramming by depleting Wdr5 before (day-5), simultaneously with (day 0) and after (day+4, +8) OSKM introduction. The most marked attenuation in iPS colony formation was observed when Wdr5 was depleted during the initial stages of reprogramming (Figure 7F). Moreover, this reduction in iPS efficiency was measurable very early (day8) in reprogramming using AP and SSEA1 as ‘surrogate’ markers of pluripotency, before endogenous Oct4 is activated (Figure 7G). This reduction was observed as late as day 20, arguing against a mere delay in reprogramming. Taken together, these data suggest that OSKM requires robust Wdr5 activity for effective somatic cell reprogramming.

## DISCUSSION

The significance of our study is three fold. First, our work represents the first detailed characterization of any core *trxG* member in the maintenance of ES cell self-renewal. *PcG*-associated members have been well-characterized in this context. Knockout ES cells for *PcG* have been established, genome-wide binding targets have been investigated in both mouse and human ES cells (Surface et al., 2010) and recently, multiple groups have performed *PcG* pull-down experiments to identify Jumonji domain proteins as critical mediators of pluripotency (Landeira and Fisher, 2010). In contrast, there exist few complementary studies for *trxG*-associated members. Although not a cell/tissue specific factor like Oct4, we observed that elevated Wdr5 expression appears to be a unique and defining property of pluripotent ES and iPS cells. Despite the identification of bivalent domains, it is unclear whether the H3K4me3 modification is required for transcriptional activation of self-renewal genes. Here, we reduced H3K4me3 levels, through the perturbation of a core *trxG* protein, and observed significant attenuation in self-renewal gene expressions that eventually leads to the induction of differentiation. Reduction, but not complete ablation, of H3K4me3 in our shRNA experiments allowed us to observe this self-renewal defect. We predict that a complete removal of Wdr5 and consequently the H3K4me3 mark, would result in a possibly lethal phenotype that bypasses self-renewal maintenance. We have provided significant data suggesting that the consequence of losing Wdr5 is, in part, mediated through the loss of H3K4me3. However, it remains possible that Wdr5 interacts with other factors, apart from Oct4, and performs functions distinct from H3K4me3 modification that also could result in loss of pluripotency.

Additionally, our data supplements published work on Chd1 and Tip60-p400 complex. Chd1 was shown to be essential for open chromatin, pluripotency and reprogramming (Gaspar-Maia et al., 2009). Their results support our findings as Chd1 is a “reader” of the H3K4me3 mark while our complementary results show Wdr5 to be a “presenter” of H3K4. We indeed observed increased expression of H3K4me3 and acetylated H3K9/14, in ES cells compared to somatic cells; which presumably maintains the ES cell epigenome in its open and transcriptionally permissive state. Fazio *et al.* reported that reduced H3K4me3 diminished Tip60-p400 recruitment to chromatin and induced loss of ES cell identity (Fazio et al., 2008). These studies, including our work, collectively indicate that the H3K4me3 mark is an indispensable histone mark that regulates the balance between self-renewal and lineage commitment.



Second, we put forward an integrated transcriptional network – epigenetic regulatory model for the maintenance of self-renewal. We and others have shown that H3K4me3 marks a large proportion of the ES cell genome including promoters unrelated to self-renewal. How then, can the self-renewal function of Wdr5/H3K4me3 be conferred? We propose that the locus specificity of Wdr5 is, in part, conferred through its direct and functional interaction with Oct4. We focused on the Oct4-Wdr5 interaction because Oct4 is a master regulator of pluripotency and is the only factor that, until recently remained irreplaceable in reprogramming (Heng et al., 2010). However, at least in some experiments we did observe co-IP of Sox2 and Nanog, suggesting that Wdr5 may interact with a more extensive complex of transcription factors. A recent study reported an Oct4-interactome of 166 proteins, which included transcription factors and chromatin-modifying complexes, many of which not previously known to associate with the ES cell network (Dejosez et al., 2010; van den Berg et al., 2010). The Wdr5-Oct4 interaction was also observed in there. Our mechanistic work on Wdr5 therefore elucidates the functional importance of this interaction and possibly sheds light on the relevance of Oct4's surprisingly broad range of interaction partners.

We also determined that *trxG* and the OSN-triad co-localize at key self-renewal regulatory genes and synergistically maintain their robust expression levels. Gene promoters that are only OSN-bound or only *trxG*-bound are less likely to be transcriptionally active in ES cells. Our genome-wide localization analyses of Wdr5 and Rbbp5 represent the first unbiased, high-resolution mapping of core *trxG* member occupancy in any cell/tissue type and thus provide a valuable resource for future investigation of *trxG*-mediated gene regulation and potential TRE-motif discovery (Table S4).

Lastly, we established that Wdr5 is required for the initial re-configuration phase of somatic cell reprogramming. We propose that the Wdr5-Oct4 partnership accomplishes this as follows (Figure 7H). First, Oct4 enhances basal Wdr5 expression in MEFs (blue arrow) through direct binding and transcriptional activation of its promoter. Next, the DNA specificity conferred by Oct4 directs Wdr5 to genomic loci encoding self-renewal genes, such as *Pou5f1* and *Nanog*, to re-establish a H3K4me3-high chromatin signature (green arrow). This elevated expression of H3K4me3 subsequently facilitates strong Oct4 occupancy to direct robust transcriptional activation (red arrow), presumably in conjunction with the larger *trxG* complex. Finally, the positive feedback loop set up by Oct4 targeting *Wdr5* (purple arrows) allows for the establishment of iPS cells or the maintenance of ES cell self-renewal. EB- and RA-differentiation or *trxG* member depletion compromises the maintenance of self-renewal and triggers differentiation.

In summary, the work presented here elucidates a previously unrecognized interconnectivity between the core transcriptional network and select members of the *trxG* complex, reveals important insights into the role of Wdr5/H3K4me3 in the maintenance of ES cell self-renewal and suggests for the first time, how Oct4 downstream target epigenetic factors re-configure the H3K4me3 signature during the process of somatic cell reprogramming.

## EXPERIMENTAL PROCEDURES

### Cell culture and differentiation assays

Mouse ES cell lines- E14T, CCE, J1, ZHBTc4, NanogR and Wdr5R were cultured and differentiated as previously described (Ivanova et al., 2006). Dermal papilla, dermal fibroblasts and MEFs were derived as described previously (Tsai et al., 2010).

### Gene expression microarray, GO and GSEA

Microarrays were conducted on Illumina Beadchip arrays. All data were normalized using LumiR. Differentially expressed genes were identified using Limma:  $\text{Log}_2\text{FC} > 0.6$  or  $< -0.6$ ;

adjusted p-value <0.05; and detection probability >0.99. Microarray data deposited at GEO (GSE19588). Cluster 3.0 and Java Treeview were used for data visualization. GO was performed at <http://www.pantherdb.org/>. GSEA was performed at <http://www.broadinstitute.org/gsea/>.

### Real-Time Quantitative PCR and Immunoblotting

Total RNA was Trizol-extracted, column-purified and reverse transcribed using the High Capacity kit (Applied Biosystems). For ChIP-qPCR analysis, 1ng ChIP-DNA was used for each PCR. All qPCR analyses performed using Fast SYBR® Green (Applied Biosystems). To obtain whole cell protein extracts, cells were lysed in RIPA buffer. Primer sequences and antibodies available in Supplemental Information.

### Short hairpin RNA design

Target sequences: Wdr5 shRNA2-GCCGTTTCATTTCAACCGTGAT, Wdr5 shRNA4-GCAAGTTCATCTGCTGATA, Oct4 shRNA-GAAGGATGTGGTTCGAGTA, Nanog shRNA-GAACTATTCTTGCTTACAA, Menin shRNA-GTAGATTTCCGCACTTTAT, Ash2l shRNA-CGAGTCTTGTTAGCCCTACAT.

### Co-IP and ChIP Assay

ES cells were lysed in Buffer-G, incubated overnight with 5ug antibody and captured with Protein G beads. Protein complexes were eluted by boiling in loading buffer. 10ul was used for each immunoblot with 2% input. Epitope-tagged co-IP in 293T cells was performed with Flag and Myc antibodies in Buffer G. ChIP performed as described previously (Schaniel et al., 2009).

### Biotinylated-peptide IP

Biotinylated peptides were synthesized and conjugated to streptavidin beads. ES cell extracts were prepared in Buffer G and incubated with peptide-conjugated beads. Beads were washed and eluted in loading buffer.

### Gel filtration and *in vitro* binding assay

Gel filtration performed in DuoFlow BioLogic System according to manufacturer's manual (Biorad). *In vitro* binding assay was conducted in Buffer G with purified Pou5f1 and Wdr5 (Origene).

### Generation of iPS cells

As described previously (Tsai et al., 2010), Oct4-GFP MEFs were transduced with pMX-Oct4, Sox2, Klf4 and cMyc retroviruses and cultured in ES media on irradiated-MEFs. GFP positive colonies were counted after 14 days post-transduction.

### ChIP-sequencing and data analysis

ChIPed DNA was blunt-ended, linker-ligated, amplified and applied to the flow-cell using the Solexa Cluster Station (Illumina). Samples were subjected to 36 cycles of sequencing using the Genome Analyzer II (Illumina). Images acquired were processed through the image extraction pipeline and aligned to mouse NCBI build mm9 using ELAND. ChIP-seq data deposited at GEO (GSE22934).

### ETOC Paragraph

Are the transcriptional and epigenetic networks in embryonic stem cells functionally integrated? What factor(s) mediate such an interaction? In this issue, Ang et al. show that Wdr5, an ‘effector’ of Histone 3 Lys-4 methylation, physically and functionally interacts with the master pluripotency regulator Oct4, for self-renewal and somatic cell reprogramming. Their findings illustrate an interconnectivity between the core transcriptional circuitry and the putative ‘histone code’, representing a direct link between the embryonic stem cell epigenome and transcriptome.

## Supplementary Material

Refer to Web version on PubMed Central for supplementary material.

## Acknowledgments

We thank C.D-Allis, C-Hughes, J-Wysocka, A-Sevilla, X-Carvajal-Vergara, F-Pereira, A-Waghray, S-Pardo, S-Mendez-Ferrer, WL-Tam, B-Lim, C-Ren, HA-Wu, J-Gingold and V-Nair for technical assistance, materials and advice. This work was supported by NIH (R01GM078465) to I.R.L. and NYSTEM (C024410) to I.R.L. and C.S., NYSTEM (C024285) to E.B. D.F.L. is a NYSCF Fellow. M.R. is supported by a Dermatology Foundation Career Development Award.

## REFERENCES

- Bernstein BE, Mikkelsen TS, Xie X, Kamal M, Huebert DJ, Cuff J, Fry B, Meissner A, Wernig M, Plath K, et al. A bivalent chromatin structure marks key developmental genes in embryonic stem cells. *Cell*. 2006; 125:315–326. [PubMed: 16630819]
- Bilodeau S, Kagey MH, Frampton GM, Rahl PB, Young RA. SetDB1 contributes to repression of genes encoding developmental regulators and maintenance of ES cell state. *Genes Dev*. 2009; 23:2484–2489. [PubMed: 19884255]
- Boyer LA, Plath K, Zeitlinger J, Brambrink T, Medeiros LA, Lee TI, Levine SS, Wernig M, Tajonar A, Ray MK, et al. Polycomb complexes repress developmental regulators in murine embryonic stem cells. *Nature*. 2006; 441:349–353. [PubMed: 16625203]
- Cao F, Chen Y, Cierpicki T, Liu Y, Basrur V, Lei M, Dou Y. An Ash2L/RbBP5 Heterodimer Stimulates the MLL1 Methyltransferase Activity through Coordinated Substrate Interactions with the MLL1 SET Domain. *PLoS One*. 2010; 5:e14102. [PubMed: 21124902]
- Carvajal-Vergara X, Sevilla A, D’Souza SL, Ang YS, Schaniel C, Lee DF, Yang L, Kaplan AD, Adler ED, Rozov R, et al. Patient-specific induced pluripotent stem-cell-derived models of LEOPARD syndrome. *Nature*. 2010; 465:808–812. [PubMed: 20535210]
- Chen X, Xu H, Yuan P, Fang F, Huss M, Vega VB, Wong E, Orlov YL, Zhang W, Jiang J, et al. Integration of external signaling pathways with the core transcriptional network in embryonic stem cells. *Cell*. 2008; 133:1106–1117. [PubMed: 18555785]
- Couture JF, Collazo E, Trievel RC. Molecular recognition of histone H3 by the WD40 protein WDR5. *Nat Struct Mol Biol*. 2006; 13:698–703. [PubMed: 16829960]
- Dejosez M, Levine SS, Frampton GM, Whyte WA, Stratton SA, Barton MC, Gunaratne PH, Young RA, Zwaka TP. Ronin/Hcf-1 binds to a hyperconserved enhancer element and regulates genes involved in the growth of embryonic stem cells. *Genes Dev*. 2010; 24:1479–1484. [PubMed: 20581084]
- Dou Y, Milne TA, Ruthenburg AJ, Lee S, Lee JW, Verdine GL, Allis CD, Roeder RG. Regulation of MLL1 H3K4 methyltransferase activity by its core components. *Nat Struct Mol Biol*. 2006; 13:713–719. [PubMed: 16878130]
- Efroni S, Duttagupta R, Cheng J, Dehghani H, Hoepfner DJ, Dash C, Bazett-Jones DP, Le Grice S, McKay RD, Buetow KH, et al. Global transcription in pluripotent embryonic stem cells. *Cell Stem Cell*. 2008; 2:437–447. [PubMed: 18462694]
- Fazio TG, Huff JT, Panning B. An RNAi screen of chromatin proteins identifies Tip60-p400 as a regulator of embryonic stem cell identity. *Cell*. 2008; 134:162–174. [PubMed: 18614019]

- Gaspar-Maia A, Alajem A, Polesso F, Sridharan R, Mason MJ, Heidersbach A, Ramalho-Santos J, McManus MT, Plath K, Meshorer E, et al. Chd1 regulates open chromatin and pluripotency of embryonic stem cells. *Nature*. 2009; 460:863–868. [PubMed: 19587682]
- Guccione E, Martinato F, Finocchiaro G, Luzi L, Tizzoni L, Dall’Olio V, Zardo G, Nervi C, Bernard L, Amati B. Myc-binding-site recognition in the human genome is determined by chromatin context. *Nat Cell Biol*. 2006; 8:764–770. [PubMed: 16767079]
- Heng JC, Feng B, Han J, Jiang J, Kraus P, Ng JH, Orlov YL, Huss M, Yang L, Lufkin T, et al. The nuclear receptor Nr5a2 can replace Oct4 in the reprogramming of murine somatic cells to pluripotent cells. *Cell Stem Cell*. 2010; 6:167–174. [PubMed: 20096661]
- Ivanova N, Dobrin R, Lu R, Kotenko I, Levorse J, DeCoste C, Schafer X, Lun Y, Lemischka IR. Dissecting self-renewal in stem cells with RNA interference. *Nature*. 2006; 442:533–538. [PubMed: 16767105]
- Karnik SK, Chen H, McLean GW, Heit JJ, Gu X, Zhang AY, Fontaine M, Yen MH, Kim SK. Menin controls growth of pancreatic beta-cells in pregnant mice and promotes gestational diabetes mellitus. *Science*. 2007; 318:806–809. [PubMed: 17975067]
- Kim J, Chu J, Shen X, Wang J, Orkin SH. An extended transcriptional network for pluripotency of embryonic stem cells. *Cell*. 2008; 132:1049–1061. [PubMed: 18358816]
- Kim J, Woo AJ, Chu J, Snow JW, Fujiwara Y, Kim CG, Cantor AB, Orkin SH. A Myc network accounts for similarities between embryonic stem and cancer cell transcription programs. *Cell*. 2010; 143:313–324. [PubMed: 20946988]
- Lairmore TC, Chen H. Role of menin in neuroendocrine tumorigenesis. *Adv Exp Med Biol*. 2009; 668:87–95. [PubMed: 20175456]
- Landeira D, Fisher AG. Inactive yet indispensable: the tale of Jarid2. *Trends Cell Biol*. 2010
- Loh YH, Zhang W, Chen X, George J, Ng HH. Jmjd1a and Jmjd2c histone H3 Lys 9 demethylases regulate self-renewal in embryonic stem cells. *Genes Dev*. 2007; 21:2545–2557. [PubMed: 17938240]
- Marson A, Levine SS, Cole MF, Frampton GM, Brambrink T, Johnstone S, Guenther MG, Johnston WK, Wernig M, Newman J, et al. Connecting microRNA genes to the core transcriptional regulatory circuitry of embryonic stem cells. *Cell*. 2008; 134:521–533. [PubMed: 18692474]
- Mikkelsen TS, Ku M, Jaffe DB, Liebman E, Giannoukos G, Alvarez P, Brockman W, Kim TK, Koche RP, et al. Genome-wide maps of chromatin state in pluripotent and lineage-committed cells. *Nature*. 2007; 448:553–560. [PubMed: 17603471]
- Pasini D, Bracken AP, Hansen JB, Capillo M, Helin K. The polycomb group protein Suz12 is required for embryonic stem cell differentiation. *Mol Cell Biol*. 2007; 27:3769–3779. [PubMed: 17339329]
- Pasini D, Cloos PA, Walfridsson J, Olsson L, Bukowski JP, Johansen JV, Bak M, Tommerup N, Rappsilber J, Helin K. JARID2 regulates binding of the Polycomb repressive complex 2 to target genes in ES cells. *Nature*. 2010; 464:306–310. [PubMed: 20075857]
- Perez-Iratxeta C, Palidwor G, Porter CJ, Sanche NA, Huska MR, Suomela BP, Muro EM, Krzyzanowski PM, Hughes E, Campbell PA, et al. Study of stem cell function using microarray experiments. *FEBS Lett*. 2005; 579:1795–1801. [PubMed: 15763554]
- Pullirsch D, Hartel R, Kishimoto H, Leeb M, Steiner G, Wutz A. The Trithorax group protein Ash2l and Saf-A are recruited to the inactive X chromosome at the onset of stable X inactivation. *Development*. 2010; 137:935–943. [PubMed: 20150277]
- Rahl PB, Lin CY, Seila AC, Flynn RA, McQuine S, Burge CB, Sharp PA, Young RA. c-Myc regulates transcriptional pause release. *Cell*. 2010; 141:432–445. [PubMed: 20434984]
- Ringrose L, Paro R. Epigenetic regulation of cellular memory by the Polycomb and Trithorax group proteins. *Annu Rev Genet*. 2004; 38:413–443. [PubMed: 15568982]
- Schaniel C, Ang YS, Ratnakumar K, Cormier C, James T, Bernstein E, Lemischka IR, Paddison PJ. Smarcc1/Baf155 couples self-renewal gene repression with changes in chromatin structure in mouse embryonic stem cells. *Stem Cells*. 2009; 27:2979–2991. [PubMed: 19785031]
- Schuettengruber B, Chourrout D, Vervoort M, Leblanc B, Cavalli G. Genome regulation by polycomb and trithorax proteins. *Cell*. 2007; 128:735–745. [PubMed: 17320510]
- Shilatifard A. Chromatin modifications by methylation and ubiquitination: implications in the regulation of gene expression. *Annu Rev Biochem*. 2006; 75:243–269. [PubMed: 16756492]

- Stoller JZ, Huang L, Tan CC, Huang F, Zhou DD, Yang J, Gelb BD, Epstein JA. Ash2l interacts with Tbx1 and is required during early embryogenesis. *Exp Biol Med (Maywood)*. 2010; 235:569–576. [PubMed: 20463296]
- Surface LE, Thornton SR, Boyer LA. Polycomb group proteins set the stage for early lineage commitment. *Cell Stem Cell*. 2010; 7:288–298. [PubMed: 20804966]
- Tam, WL.; Lim, CY.; Han, J.; Zhang, J.; Ang, YS.; Ng, HH.; Yang, H.; Lim, B. *Stem cells*. Ohio: Dayton; 2008. Tcf3 Regulates Embryonic Stem Cell Pluripotency and Self-Renewal by the Transcriptional Control of Multiple Lineage Pathways.
- Tay YM, Tam WL, Ang YS, Gaughwin PM, Yang H, Wang W, Liu R, George J, Ng HH, Perera RJ, et al. MicroRNA-134 modulates the differentiation of mouse embryonic stem cells, where it causes post-transcriptional attenuation of Nanog and LRH1. *Stem Cells*. 2008; 26:17–29. [PubMed: 17916804]
- Taylor MD, Sadhukhan S, Kottangada P, Ramgopal A, Sarkar K, D'Silva S, Selvakumar A, Candotti F, Vyas YM. Nuclear role of WASp in the pathogenesis of dysregulated TH1 immunity in human Wiskott-Aldrich syndrome. *Sci Transl Med*. 2010; 2 37ra44.
- Thomson JP, Skene PJ, Selfridge J, Clouaire T, Guy J, Webb S, Kerr AR, Deaton A, Andrews R, James KD, et al. CpG islands influence chromatin structure via the CpG-binding protein Cfp1. *Nature*. 2010; 464:1082–1086. [PubMed: 20393567]
- Tsai SY, Clavel C, Kim S, Ang YS, Grisanti L, Lee DF, Kelley K, Rendl M. Oct4 and klf4 reprogram dermal papilla cells into induced pluripotent stem cells. *Stem Cells*. 2010; 28:221–228. [PubMed: 20014278]
- Tyagi S, Herr W. E2F1 mediates DNA damage and apoptosis through HCF-1 and the MLL family of histone methyltransferases. *EMBO J*. 2009; 28:3185–3195. [PubMed: 19763085]
- van den Berg DL, Snoek T, Mullin NP, Yates A, Bezstarosti K, Demmers J, Chambers I, Poot RA. An Oct4-centered protein interaction network in embryonic stem cells. *Cell Stem Cell*. 2010; 6:369–381. [PubMed: 20362541]
- Wang P, Lin C, Smith ER, Guo H, Sanderson BW, Wu M, Gogol M, Alexander T, Seidel C, Wiedemann LM, et al. Global analysis of H3K4 methylation defines MLL family member targets and points to a role for MLL1-mediated H3K4 methylation in the regulation of transcriptional initiation by RNA polymerase II. *Mol Cell Biol*. 2009; 29:6074–6085. [PubMed: 19703992]
- Wysocka J, Swigut T, Milne TA, Dou Y, Zhang X, Burlingame AL, Roeder RG, Brivanlou AH, Allis CD. WDR5 associates with histone H3 methylated at K4 and is essential for H3 K4 methylation and vertebrate development. *Cell*. 2005; 121:859–872. [PubMed: 15960974]
- Zhu ED, Demay MB, Gori F. Wdr5 is essential for osteoblast differentiation. *J Biol Chem*. 2008; 283:7361–7367. [PubMed: 18201971]



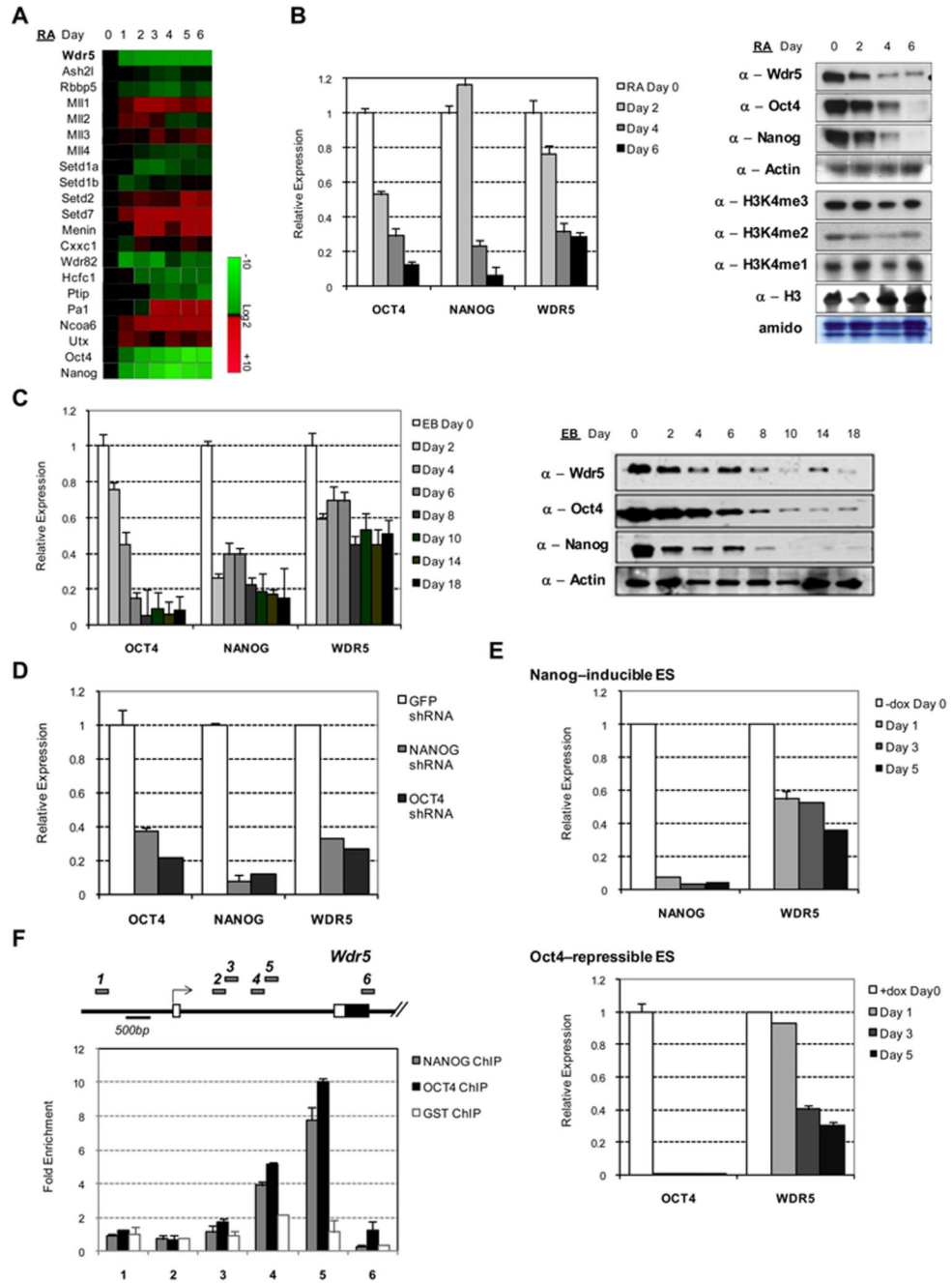


**Figure 1. Down-regulation of *Wdr5* expression upon ES cell differentiation**

(A) Heatmap of *trxG*-associated member expressions during RA-induction from (Ivanova et al., 2006)

(B, C) Real-time PCR (left) and immunoblot (right) analyses during RA-induction and EB-formation.

(D) Real-time PCR analysis after 3 days shRNA knockdown of Nanog, Oct4.

(E) Real-time PCR analysis in Nanog-inducible (Ivanova et al., 2006), Oct4-repressible lines (Schaniel et al., 2009). All data normalized to actin and shown relative to Day0 or GFP shRNA.

(F) ChIP-qPCR analysis of Oct4, Nanog occupancy at *Wdr5* locus. Numbered grey bars denote primer locations. Glutathione *S*-transferase (GST) ChIP as negative control. Values expressed as Fold Enrichment relative to input DNA and a control region (Loh et al., 2007). Data represented as mean  $\pm$  s.d, n=3. See also Figure S1.

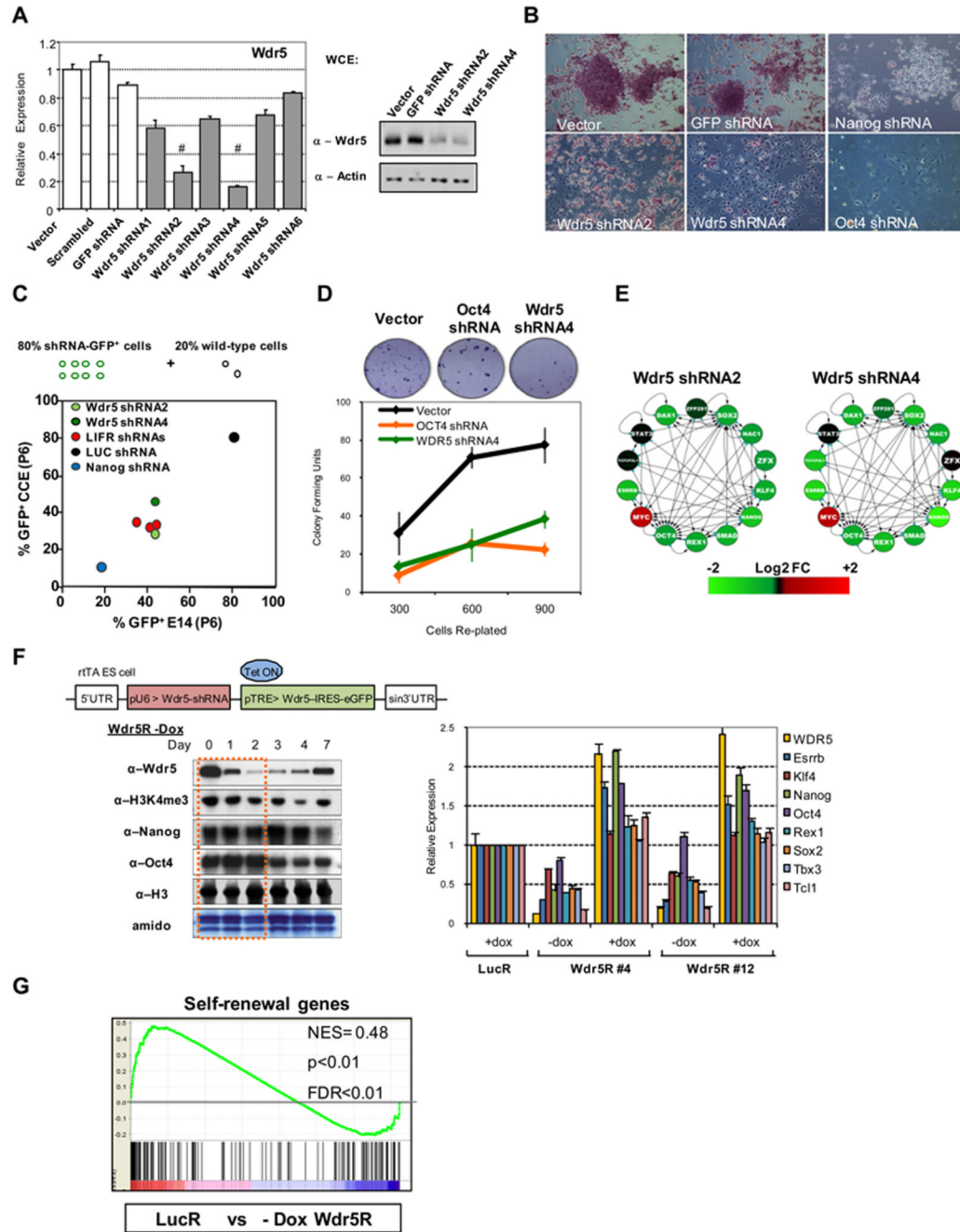


**Figure 2. Wdr5 depletion resulted in loss of self-renewal and collapse of extended transcriptional network**

(A) Real-time PCR (left) and immunoblot (right) analyses after 4 days Wdr5 knockdown  
 (B) AP staining after 4 days shRNA knockdown.  
 (C) ES cell competition assay (Ivanova et al., 2006) in E14 and CCE cells. Luciferase (LUC), Nanog and LIFR shRNAs serve as negative and positive controls respectively.  
 (D) Secondary ES colony re-plating assay (Tay et al., 2008). Circles depict colonies from the 600 cell-replated wells.

(E) Gene expression of composite transcriptional network (Chen et al., 2008; Kim et al., 2008) after 4 days Wdr5-depletion as measured by real-time PCR. Log<sub>2</sub> fold change relative to GFP shRNA.

(F) Scheme of tetracycline-inducible Wdr5-rescue construct (top). Immunoblot analysis after Dox withdrawal in Wdr5R #4 (left). Orange box shows H3K4me3-reduction preceding the loss of Oct4, Nanog. Real-time PCR analysis (right) after 5 days Wdr5 knockdown (-dox) or with rescue (+dox) in two clones (Wdr5R#4,#12). All data normalized to actin and shown relative to Vector, GFP shRNA or Luc rescue clone (LucR). Data represented as mean ± s.d, n=3.

(G) GSEA of a geneset representing self-renewal markers upon Wdr5 knockdown. NES = normalized enrichment score; p= nominal p-value; FDR= false discovery rate. See also Figure S1 and S2.

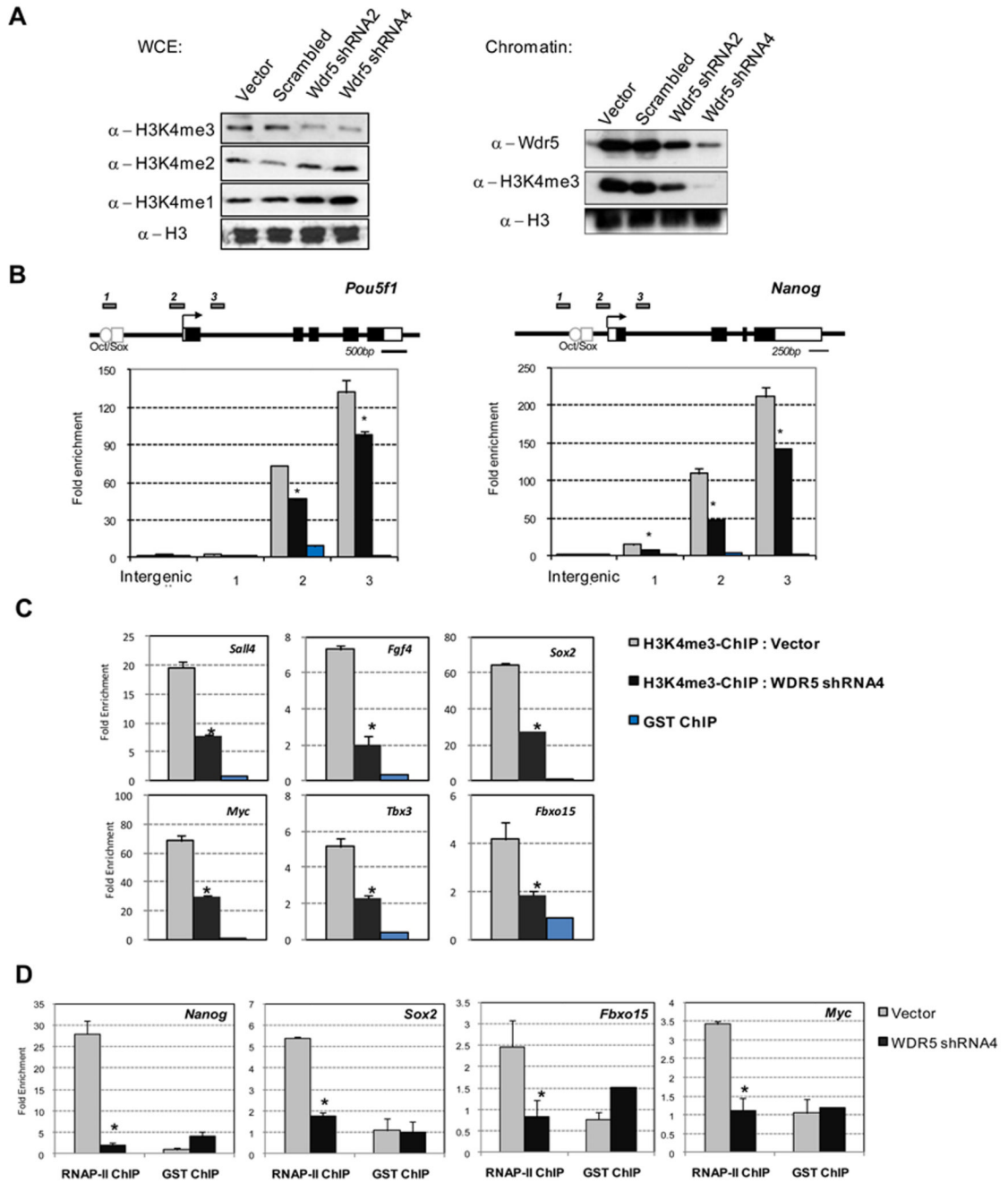


**Figure 3. Wdr5 maintains global and localized H3K4 tri-methylation**

(A) Immunoblot after 4 days Wdr5 knockdown. Whole cell extract (WCE).

(B, C) ChIP-qPCR analysis of H3K4me3 mark at various loci after Wdr5 knockdown. Numbered grey bars denote primer locations.

(D) ChIP-qPCR analysis of RNAP-II localization at various loci after Wdr5 knockdown. Values expressed as Fold Enrichment relative to input DNA and a control region. All data represented as mean ± s.d., n=3, \*P <0.005. See also Figure S3



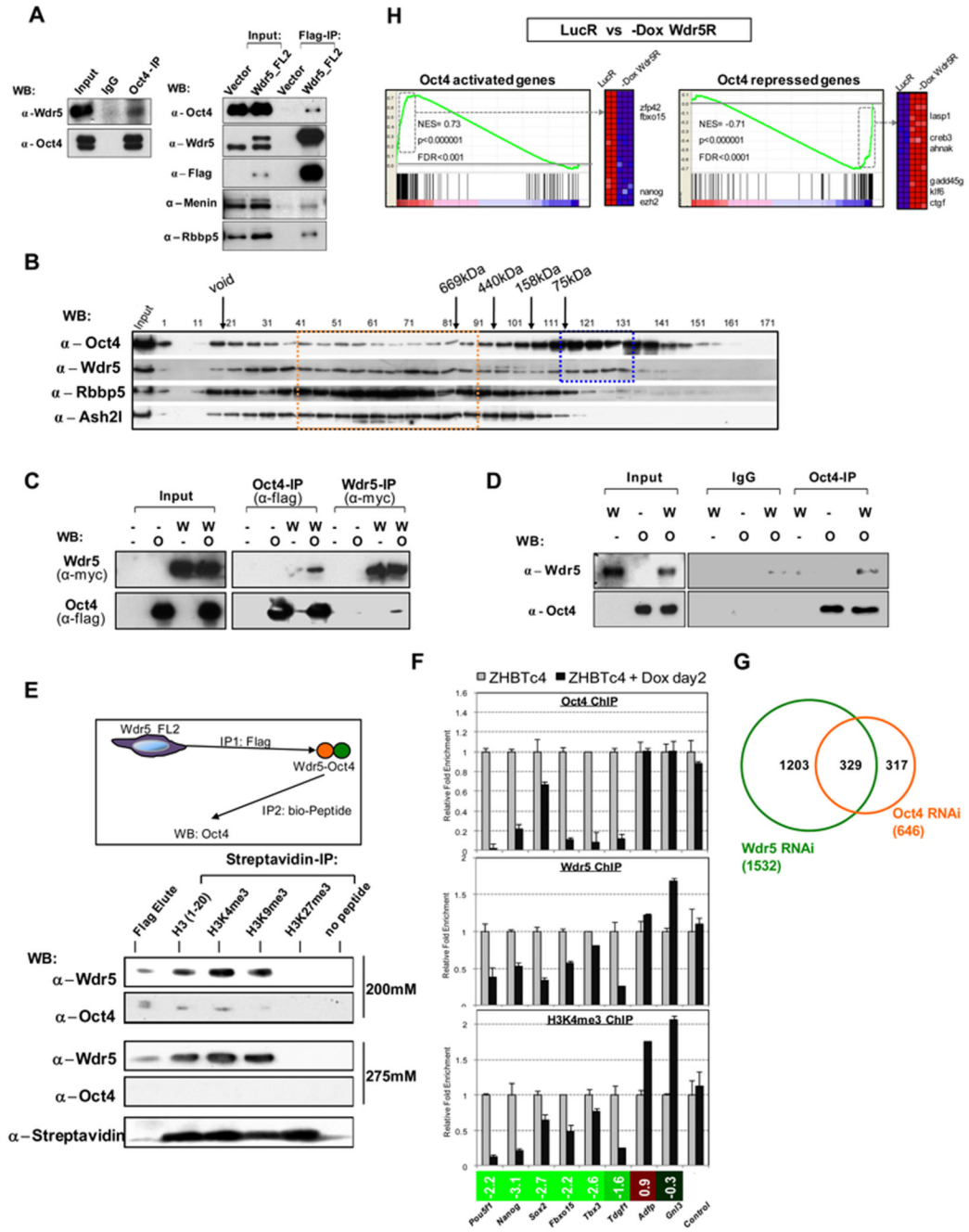


**Figure 4. Oct4 interacts with Wdr5 and share overlapping gene regulatory functions**  
 (A) Co-IP show Oct4 interaction with Wdr5. Oct4 pulldown of Wdr5 protein (left). Flag was used to IP for Wdr5 in Wdr5\_FL2 line (right). IP was repeated 3 times.  
 (B) Gel-filtration analysis of ES cell nuclear extracts. Migration of molecular markers is indicated above the panels and immunoblot antibodies shown on the left.  
 (C) Epitope-tagged co-IP in 293T cells. Flag-Oct4 (O) pulled-down Myc-Wdr5 (W), and vice versa. Flag/myc antibodies used for both IP and WB. Input shows equal expression.  
 (D) *in vitro* binding assay using recombinant Oct4 (O) and Wdr5 (W). Proteins were immunoblotted after IP with Oct4 antibody.

(E) Sequential Peptide IP assay. Flag-mediated IP of Wdr5-Oct4 complex (IP1) then biotin-peptide-mediated IP (IP2) show Oct4 specificity for H3K4me3 peptide. IP2 performed in 200mM or 275mM salt. Lane-1 (Flag Elute) is protein extract before IP2. H3(1–20) represents first 20 amino acids on unmodified H3. Streptavidin blot shows equal peptides IP'ed.

(F) ChIP-qPCR analysis of Oct4-, Wdr5-binding and H3K4me3 levels after 2 days Oct4-depletion. Values expressed as Fold Enrichment relative to ZHBTc4. *Control* denotes intergenic region bound neither by Wdr5 nor Oct4. Heatmap shows  $\text{Log}_2$  expression of genes upon Oct4-depletion. All data represented as mean  $\pm$  s.d., n=3.

(G) Venn diagram of differentially-expressed genes in Wdr5- and Oct4-depleted ES cells. P-value for overlap as computed using Monte Carlo simulation is  $<1e^{-08}$ .

(H) GSEA analyses of two gene-sets representing Oct4-activated (left) and Oct4-repressed (right) genes. Heatmap represents top enriched genes. (red= high expression; blue=low). Note similarity to Figure S5A. See also Figure S4 and S5.

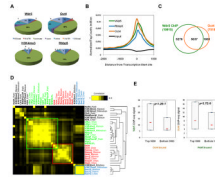


**Figure 5. Genome-wide mapping of Wdr5, Oct4, H3K4me3, and Rbbp5 localizations using ChIP-seq**

(A) Percentage distribution of ChIP-seq binding regions relative to nearest Refseq genes for Wdr5, Rbbp5, H3K4me3 and Oct4.

(B) Distributions of Rbbp5, Wdr5 and Oct4 sequence-tags relative to the transcription start site of 26412 RefSeq genes. Tag counts were normalized to total number of tags in each sequencing reaction.

(C) Venn diagram showing overlap of Wdr5 (green) and Oct4 bound (orange) genes.

(D) Heatmap of co-localization frequency of Wdr5, Rbbp5, H3K4me3 and Oct4 binding regions with published datasets (Bilodeau et al., 2009; Chen et al., 2008; Marson et al., 2008; Mikkelsen et al., 2007; Pasini et al., 2010; Rahl et al., 2010). Factors were hierarchically-clustered using average-linkage metric along both axes.

(E) Boxplots show median (red bar), 25<sup>th</sup> and 75<sup>th</sup> percentile number of ChIP-seq tags. Blue bar show 2.5<sup>th</sup> and 97.5<sup>th</sup> percentile. See also Figure S6.

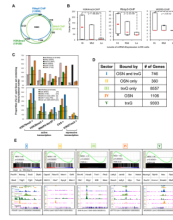


**Figure 6. Oct4, Sox2, Nanog and *trxG* are partners in transcriptional activation**

(A) Venn diagram showing overlap of Wdr5-, Rbbp5-, H3K4me3- ChIP target genes.

(B) 18096 Refseq genes were divided equally into 3 expression-groups and plotted against each ChIP-seq tag signals. Boxplots show median (red bar), 25<sup>th</sup> and 75<sup>th</sup> percentile number of ChIP-seq tags. Whiskers show 2.5<sup>th</sup> and 97.5<sup>th</sup> percentile.

(C) Proportion (%) of each geneset (colored bars), extracted from published (Chen et al., 2008; Marson et al., 2008) and current ChIP-seq datasets, containing markers of active and repressive transcription. Wdr5, Rbbp5, H3K4me3 co-bound (*trxG*). All Refseq (grey bar, black-dotted line) genes represents baseline %.

(D) Chart showing number of *trxG* and OSN bound genes sub-classified into five sectors. [I]=OSN & *trxG*, [II]=OSN without *trxG*, [III]=*trxG* without OSN, [IV]=OSN\_all, [V]=*trxG*\_all.

(E) Table containing GSEA (top-row) of mRNA expressions upon EB-differentiation (Perez-Iratxeta et al., 2005), representative gene names (middle-row) and ChIP-seq binding profiles (bottom-row) for genes in sectors [I]–[V]. See also Figure S6.

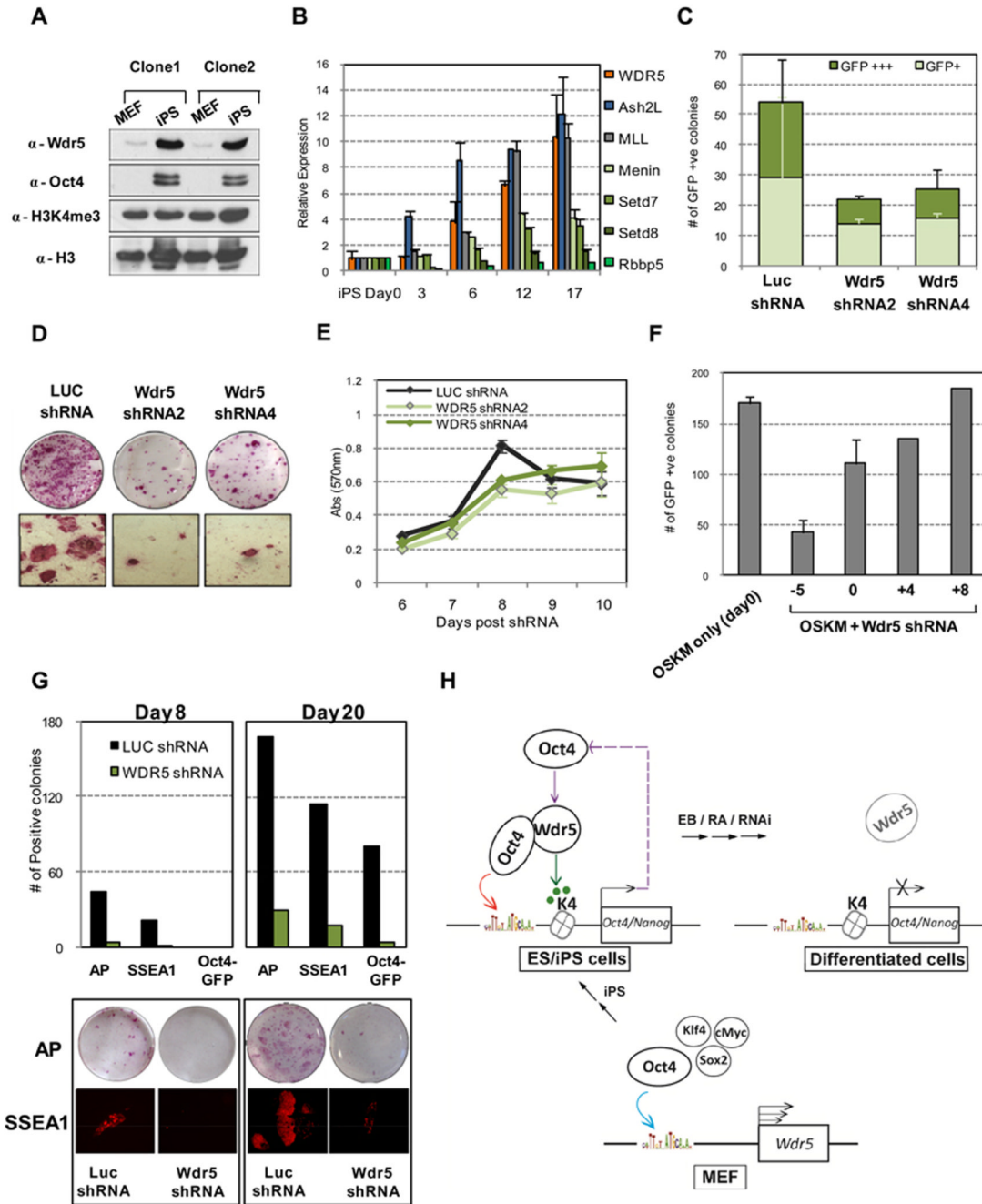


**Figure 7. Increased Wdr5 expression is required for reprogramming of Oct4-GFP MEFs by defined factors**

(A) Immunoblot of two independent iPS clones and their parental MEFs.  
 (B) Real-time PCR of *trxG*-associated members during iPS induction. Data normalized to actin and shown relative to MEF. Data represented as mean  $\pm$  s.d., n=3.  
 (C) High and low GFP positive colonies were counted 14 days post-OSKM in Wdr5- and Luc-knockdown cells. Data represented as mean  $\pm$  s.d.  
 (D) AP staining of entire wells (circles) and representative colonies (squares) from Wdr5- and Luc- knockdown iPS colonies at Day 14.  
 (E) MTT proliferation assay of MEF transduced with Luc or Wdr5 shRNA.



(F) Wdr5-depletion during iPS reprogramming. GFP<sup>+++</sup> colonies counted at Day 14. OSKM only did not receive Wdr5-shRNA.

(G) AP, SSEA1 and GFP intensity assessed at early (Day 8) or late stages (Day 20) of iPS induction with (green bar) or without (black bar) Wdr5-shRNA. AP staining of entire wells (circles) and representative SSEA1 colonies (squares) depicted.

(H) Proposed model. See also Figure S7.